Science Advances
AAAS

advances.sciencemag.org/cgi/content/full/6/26/eabc0251/DC1

Supplementary Materials for

Soft electromagnetic actuators

Guoyong Mao*, Michael Drack, Mahya Karami-Mosammam, Daniela Wirthl, Thomas Stockinger, Reinhard Schwödiauer, Martin Kaltenbrunner*

*Corresponding author. Email: guoyong.mao@jku.at (G.M.); martin.kaltenbrunner@jku.at (M.K.)

Published 26 June 2020, *Sci. Adv.* **6**, eabc0251 (2020)
DOI: 10.1126/sciadv.abc0251

The PDF file includes:

Other Supplementary Material for this manuscript includes the following:

(available at advances.sciencemag.org/cgi/content/full/6/26/eabc0251/DC1)

Fatigue test

To show the durability and stability of our SEMAs, we conducted fatigue tests with a single-coil SEMA by applying a 1 A square wave current @ 5 Hz for 60 hours at room temperature. During each period, the SEMA bends twice (left and right) to a maximum rotation angle of 61° meaning that the SEMA achieves 2.16 million bending cycles. In Fig. 2F, the voltage is not strictly a square wave because of the change in resistance under deformation (Fig. S6E) and of the electromotive force induced by the liquid metal coils passing the magnetic field.

Force estimation

To illustrate the calculation, we plotted a schematic diagram of the single-coil square SEMA (Fig. S5A&B). The SEMA is positioned centrally on the magnet surface (Fig. 1). We only consider the horizontal liquid metal channels that are subjected to the horizontal Lorentz forces bending the SEMA. There are eleven horizontal channels in the SEMA which are labeled from 1 to 11. The total moment caused by the Lorentz force can be calculated as $M = \sum_{i=1}^{i=11} B_i I l_i Z_i$, where, i is the label of the horizontal channels and Z is the distance from the channel to the magnet surface. If we apply a force F to the center of the SEMA between channels 6 and 7, we get an equilibrium force equation, $F = 2M / \left(Z_6 + Z_7 \right)$. According to Table S2, when applying a 3 A current (DC), we obtain a force $F = 0.04$ N. Our power tests conducted on the double-coil square SEMA result in a maximum force output of $F = 0.08$ N for a straight-up position of the SEMA (Fig. S5A&B).

Voltage and current measurement

We use a multifunction DAQ device (USB-6212, National Instruments) and a shielded connector block (BNC-2110, National Instruments) to obtain voltage and current of the SEMA. The current is measured via the voltage drop at a single-ohm shunt resistor (HS150 1R J, Arcol) connected in series to the SEMA. Automatic recording is performed by LabVIEW (National Instruments). The resistance of the SEMA is calculated as voltage divided by current.

Temperature measurement and heat power

The measurement was conducted in a temperature-controlled room (25 ^{o}C). For the static test, the SEMA is sourced with a current but not placed in a magnetic field. A thin and light-weight type-k thermocouple (Nr. 397-1589, RS Pro) is bonded centrally on the SEMA surface (one side). Additionally, an infrared camera (A325sc, FLIR) is used to record the temperature distribution of the whole SEMA with a sample rate of 1 Hz. For the dynamic test, the SEMA is driven by a 1 Hz square wave current with different amplitudes of 1, 2 and 3 A. In this experiment the temperature is only measured with the thermocouple. We find that the maximum (equilibrium) temperatures for 1, 2, and 3 A current are: 29 °C, 41 °C and 58 °C for the static test at the surface (Fig. 2D), 30 °C, 45 °C, and 65 °C in the core (Fig. S6C) and 29 °C, 38 °C and 46 °C for the dynamic test at the surface (Fig. S6D). The measured resistance of 0.18 ohm of the single-coil SEMA is stable under deformation. When sourcing a current of 3 A, the change in resistance is less than 2.5% compared to its reference state (Fig. S6E), where the maximum principal strain is about 10% (Fig. S6F).

The heat power $P_{heat} = I^2R$ is 1.62 W at 3 A, which can be used as a design rule for the same geometry of the SEMA.

Strain energy estimate

We assume that the current passes only the top horizontal channel of the SEMA (Fig. S6B) and treat the whole SEMA as a linear elastic beam under pure bending. Consequently, the strain energy of the SEMA can be calculated as $W = F^2 l^3 / (6EI_b)$, where F is the Lorentz force, l is the length of the beam, I_b is the moment of inertia of the beam, and E is the elastic modulus of the beam. Inserting $F \sim BI$, where B is the magnetic field strength and I is the current, results in $W \sim B^2 I^2$. Considering the limitation of P_{heat}, the maximum strain energy of the SEMA can be written as $W \sim B^2 P_{heat} / R$ so that $W_{\max} \sim B^2 / R$.

When taking the turns of the liquid metal coils n into account, the Lorentz force can be expressed as $F = nBIl$. We assume a single liquid metal channel that is equally split into n parts of the same length with the volume held constant. For n coils, the total resistance is $R_n = n^2 R$ and the power is $P_{nheat} \sim n^2 RI$. Thus, the maximum strain energy is independent of the number of turns n: $W_{\max} \sim B^2 / R$.

Power and efficiency measurement

The SEMA is connected to a weight by a cotton thread via a deflection pulley (Fig. 3A) and driven by a sine wave current at 1 Hz with different amplitudes between 1 and 3 A. The mass of the SEMA and the load are $m_a = 10.68\,\text{g}$ and $m_w = 7.32\,\text{g}$, respectively. We

use a camera (Canon EOS 80D) to capture the movement of the weight with a 50 Hz frame rate. To get the relationship between the displacement of the weight and the time, we use video analysis software (Tracker). With polynomial interpolation, we obtain a fit curve of the displacement as a function of time. Differentiation of the obtained displacement curves yields the velocity. Similarly, the second derivative gives the acceleration.

In the experiment, we apply a -3 A current first and then slowly change it to +3 A. The deflection of the SEMA from one side to the other side lifts the weight 2 cm up, which does a work of 1.4 mJ to the load (Fig. 3A). When quickly switching the current from -3 A to +3 A, we obtain the displacement *vs.* time curve presented in Fig. 3B. The maximum displacement due to such actuation is larger than 2 cm with a maximum speed of the load of 558 mm/s (Fig. 3C). By deriving the velocity, we obtain the acceleration *a* and the force in the thread equals $m_w(g+a)$ with g ($g = 9.8\,\mathrm{m/s^2}$) being the gravitational acceleration. By multiplying the resulting force and velocity, we obtain the mechanical power output of the SEMA presented in Fig. 3D.

Efficiency and power estimate

Let's consider a liquid metal channel in the magnetic field B, according to Faraday's law the electromotive force (emf) is equal to $\varepsilon = Blv$, where *l* is the length of the liquid metal channel and *v* the velocity perpendicular to the magnetic field *B*. The output power can be expressed as $P_{out} = Blv$, and the input power is $P = I^2R + \varepsilon I$. The efficiency is given by $\eta = P_{out} / P$, which can be simplified as $\eta = 1/(1 + IR/Blv)$. The resistance of the double-coil square SEMA is about 0.35 Ω. The current used is 3 A and the length of the liquid metal channel is 40 mm. The average magnetic field in the experiment is 200 mT and the

maximum velocity is about 0.5 m/s (Fig. 3C) which results in an efficiency of $\eta_{es} = 0.38\%$. For the estimation, we assume that the top horizontal channel of length l and mass m, moves a distance d along the direction of the Lorentz force by rotating from 90° to 0°. As one end of the SEMA is fixed, the distance d is smaller than the height of the SEMA. For simplification, we can take d as the height of the SEMA. The Lorentz force linearly increases from 0 to BIl, resulting in the work $1/2BIld$. If we assume that all the work done by the Lorentz force is transferred into kinetic energy ($1/2mv^2$), the velocity of the channel is $v = \sqrt{BIld/m}$. By substituting $v = \sqrt{BIld/m}$ into P_{out}, we will have $P_{out} = BIlv = (BIl)^{3/2}\sqrt{d/m}$ or $P_{out} = (BI)^{3/2}k^{-1}$, $k = \sqrt{m/dl^3}$ which is related to the mass and geometry of the liquid metal channel. When only amplifying the magnetic field to 7 T, we get the new P_{out} which is $35^{3/2}$=207.06 times of the original value. Here, we neglect the gravitational potential energy (small value, Fig. S6A) and the strain energy stored in the elastomer which is from the work of the Lorentz force. Therefore, we have a new relationship for the efficiency, $\eta = 1/\left(1 + IR/lB\sqrt{BIld/m}\right) = 1/\left(1 + \sqrt{mIR^2/dl^3B^3}\right)$, or $\eta = 1/\left(1 + k\sqrt{IR^2/B^3}\right)$. For $\eta_{es} = 0.38\%$ mentioned above, we obtain $k\sqrt{IR^2/B^3} = 262.16$. So, for $B = 7\ \mathrm{T}$ the efficiency increases to $\eta = 1/(1 + 262.16/\sqrt{35^3}) = 44.1\%$ according to the equation.

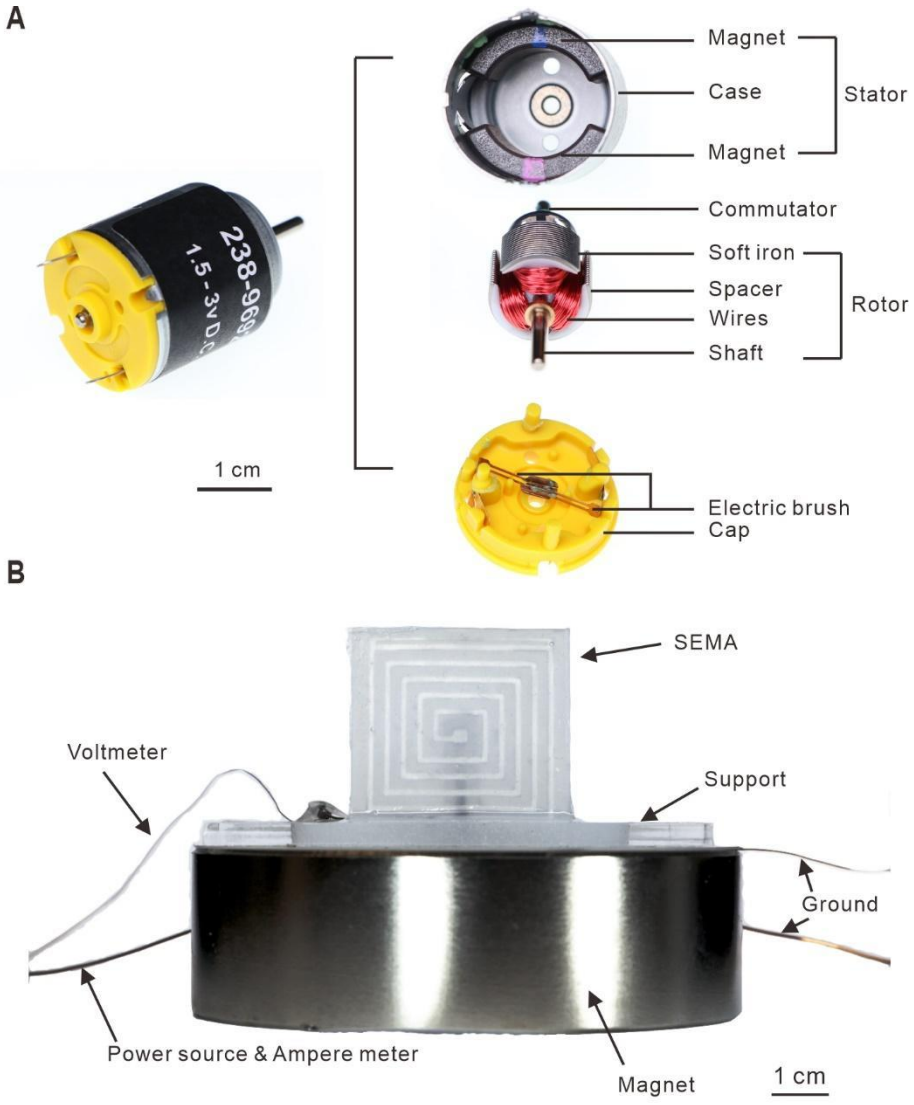

Fig. S1. Structural comparison between a conventional DC motor and a SEMA. (**A**) Disassembly diagram of a conventional DC motor. (**B**) Experimental setup of a typical SEMA (a single-coil square SEMA). (Photo Credit: Michael Drack and Guoyong Mao/Johannes Kepler University Linz).

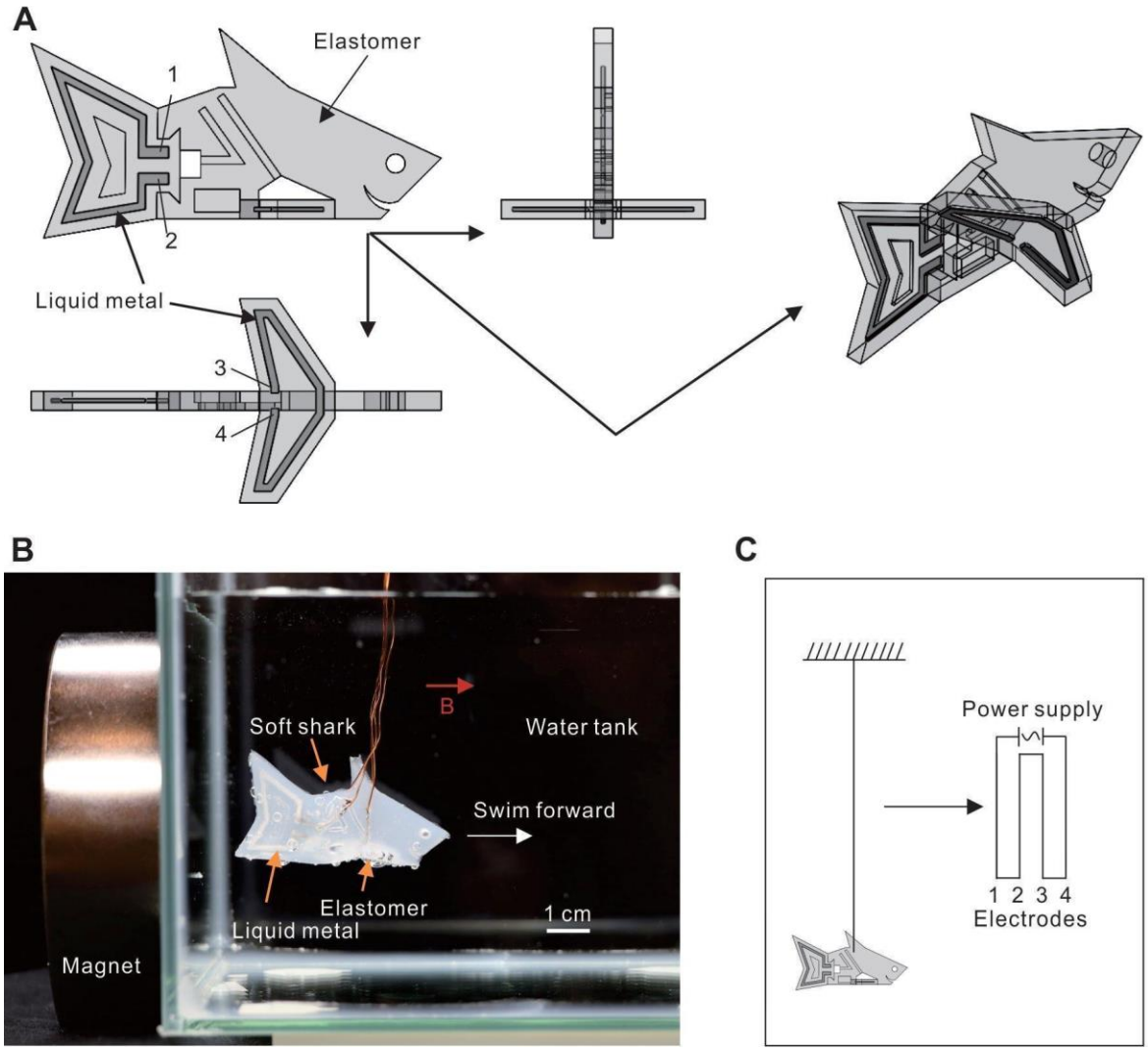

Fig. S2. A swimming soft shark driven by two SEMAs. (**A**) Structural design and assembly of the soft shark fabricated from elastomer and liquid metal. The inserted numbers indicate the connecting sites at the two ends of the liquid metal channels. (**B**) Experimental setup of the swimming soft shark (Movie S1). (**C**) The height level of the soft shark is kept constant by the mounted electrodes which are connected in series. The numbers indicate the labeling of the electrodes introduced in (A). (Photo Credit: Michael Drack and Guoyong Mao/Johannes Kepler University Linz).

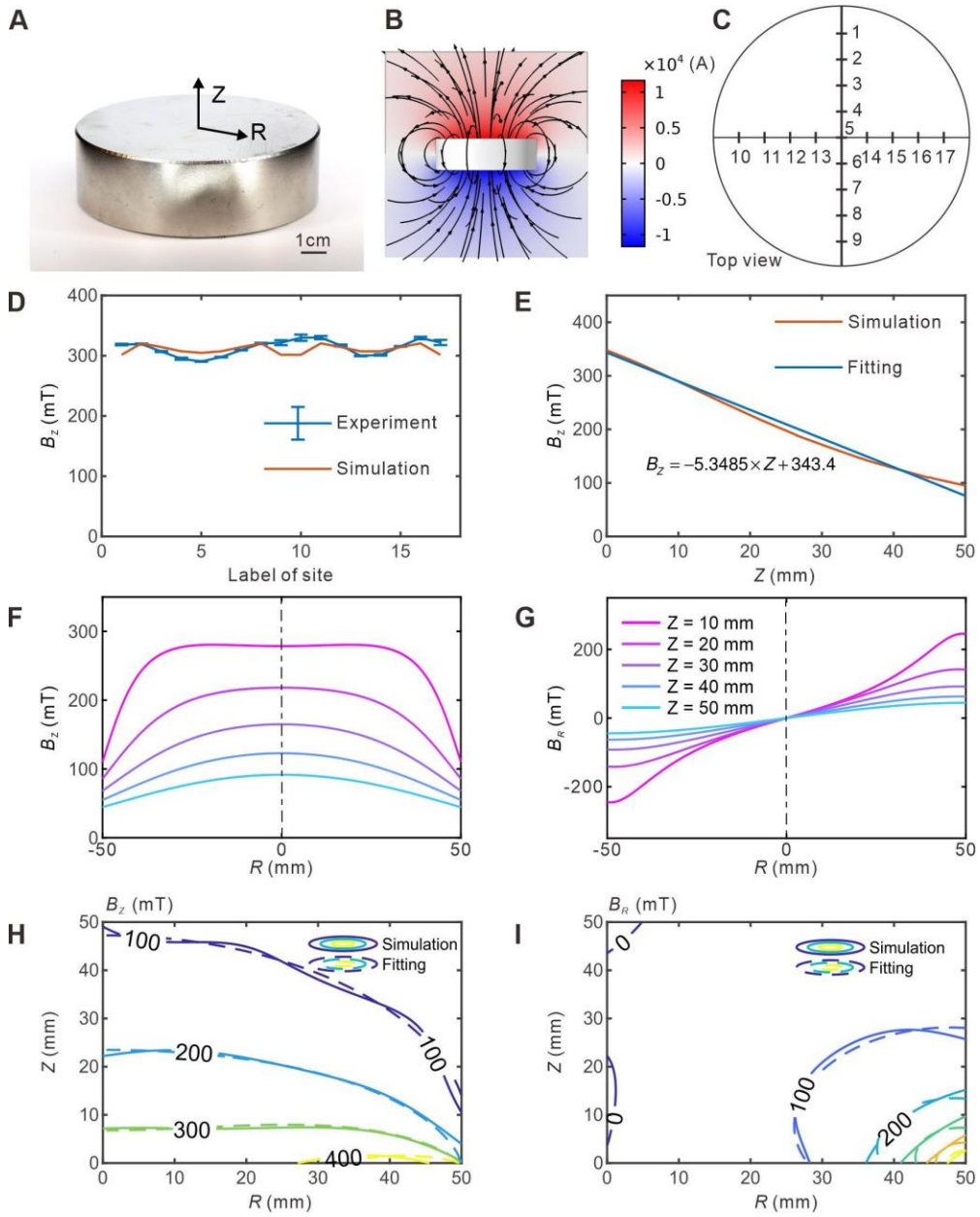

Fig. S3. Characterization of a plate magnet. (**A**) Picture of the plate magnet. (**B**) Simulated spatial distribution of the magnetic field around a plate magnet. The legend shows the strength of the magnetic potential. (**C**) Measurements of the magnetic field were taken at the labeled sites 6 mm above the surface of the magnet. (**D**) Comparison of magnetic flux density between the experimental measurement and the simulation corresponding to the labeled sites in (C). (**E**) Simulated and fitted magnetic flux density along the symmetry axis of the magnet at R=0. (**F**&**G**) Distribution of the two components of the magnetic field at different heights Z above the surface of the magnet. (**H**&**I**) Contour maps of a 3D numerical fitting of the magnetic field on the top of the plate magnet compared with the simulated results. (Photo Credit: Michael Drack and Guoyong Mao/Johannes Kepler University Linz).

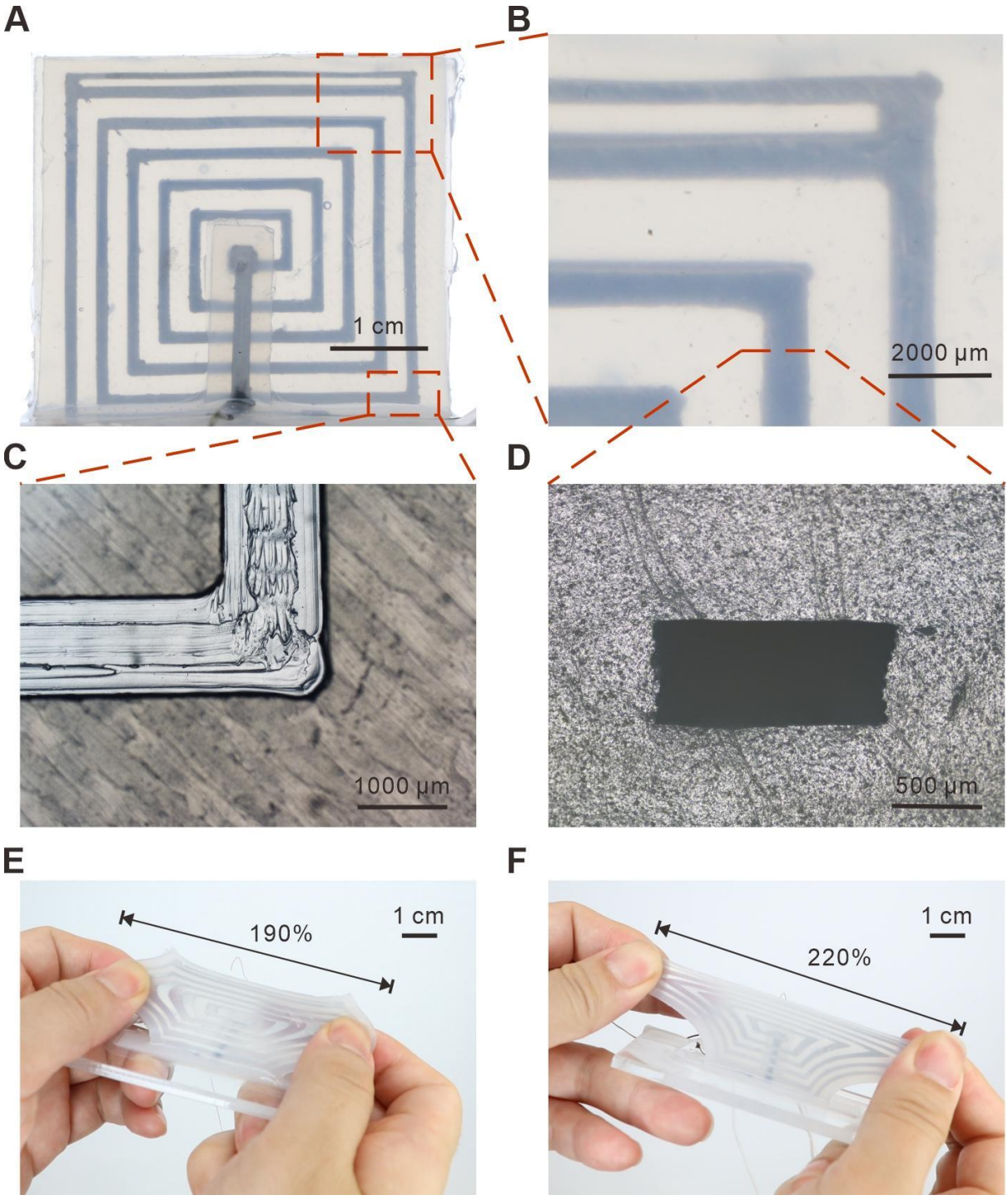

Fig. S4. Verification of fabrication quality. (**A**) Overall view of a single-coil square SEMA. (**B**) Detail of the top corner with liquid metal filled channels. (**C&D**) In-plane and out-of-plane cross-sectional views of the channels. (**E&F**) Stretching a single-coil square SEMA proofs the precisely sealed liquid channels (Movie S2). The SEMA is stretched to 190% and 220% in (E) and (F), respectively. (Photo Credit: Michael Drack and Guoyong Mao/Johannes Kepler University Linz).

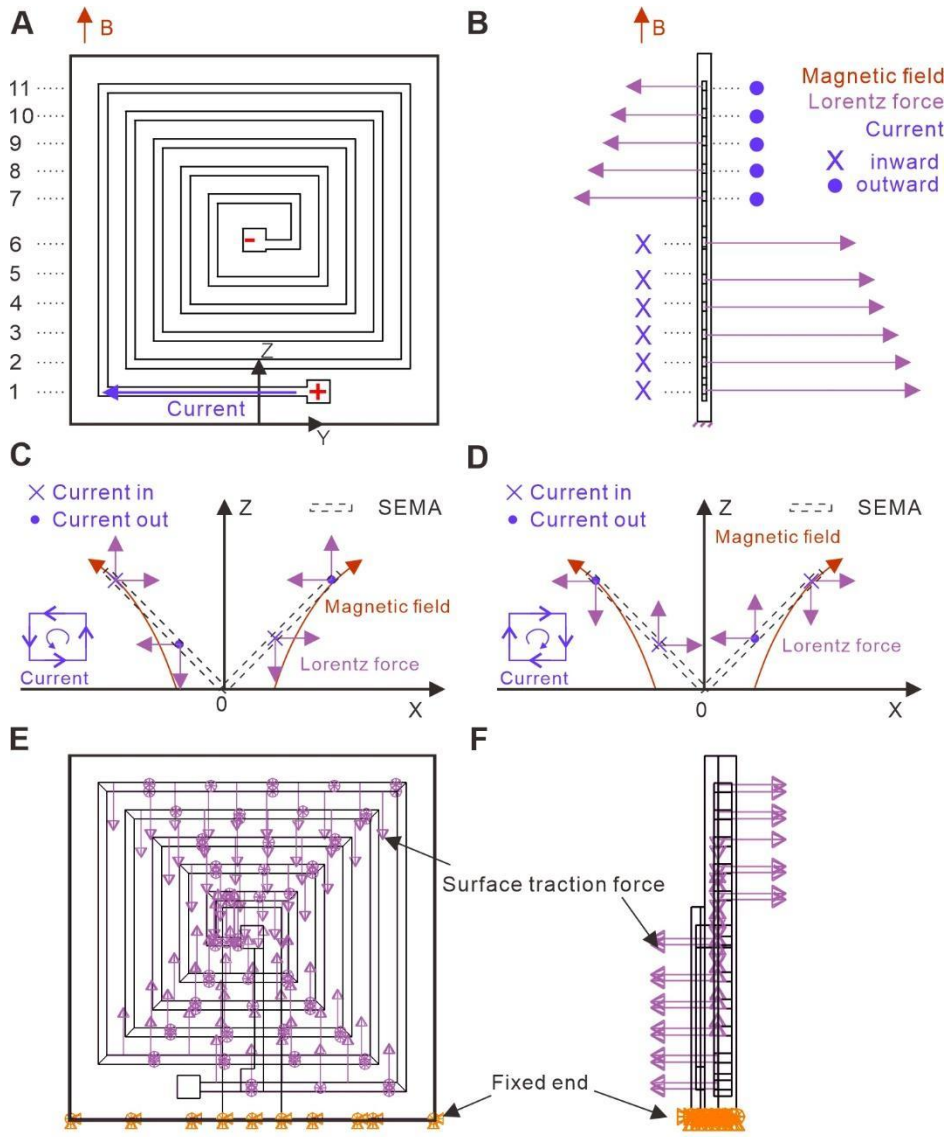

Fig. S5. Principle and numerical model of the SEMA. (**A**) Schematic illustration of the single-coil square SEMA with numbered horizontal channels. (**B**) Schematic diagram of the distribution of the horizontal component of the Lorentz force which is decreasing with increasing height as a consequence of the decaying magnetic field strength. (**C**&**D**) Directions of the Lorentz force in a curved single-coil SEMA with the clockwise and counterclockwise current direction. (**E**&**F**) The applying load of a single-coil square SEMA in simulation from the front and side views, respectively.

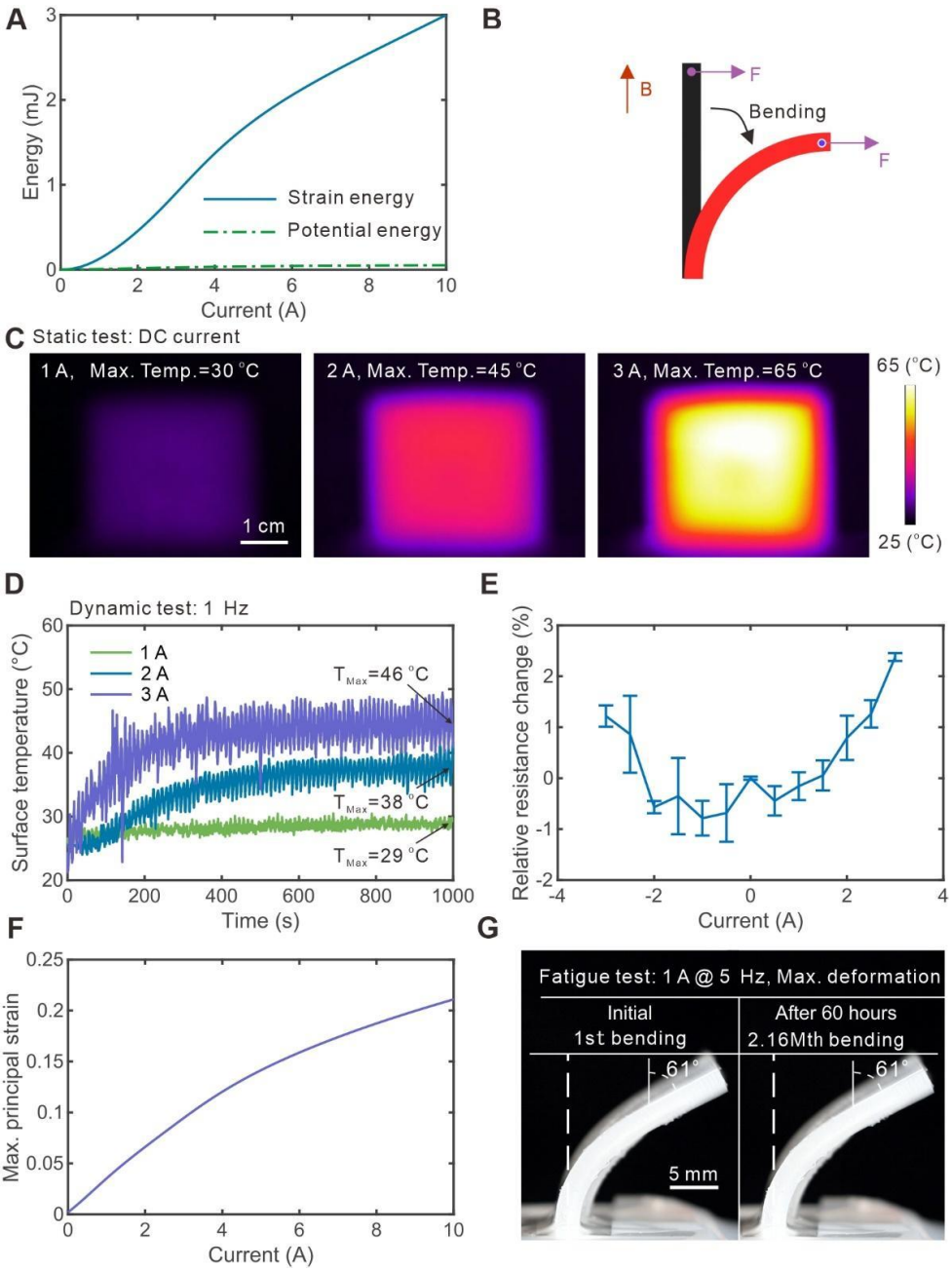

Fig. S6. Characterization of a single-coil square SEMA. (**A**) Strain and potential energy *vs.* current of the SEMA. The potential energy is equal to the gravitational potential energy. (**B**) A schematic model of a single-coil square SEMA in a pure bending state by applying a Lorentz force. (**C**) Equilibrium state of the temperature distribution of the SEMA subjected to a current of 1, 2 and 3 A recorded by an infrared camera. (**D**) Temporal change in the temperature of the SEMA subjected to a 1 Hz square wave current with an amplitude from 1 to 3 A. (**E**) Resistance change of the SEMA subjected measured for different currencies. (**F**) Simulated maximum principal strain *vs.* current of the SEMA. (**G**) The maximum bending angle of the SEMA subjected to a square wave current of 1 A @ 5 Hz before and after 2.16 million bending cycles. (Photo Credit: Michael Drack and Guoyong Mao/Johannes Kepler University Linz).

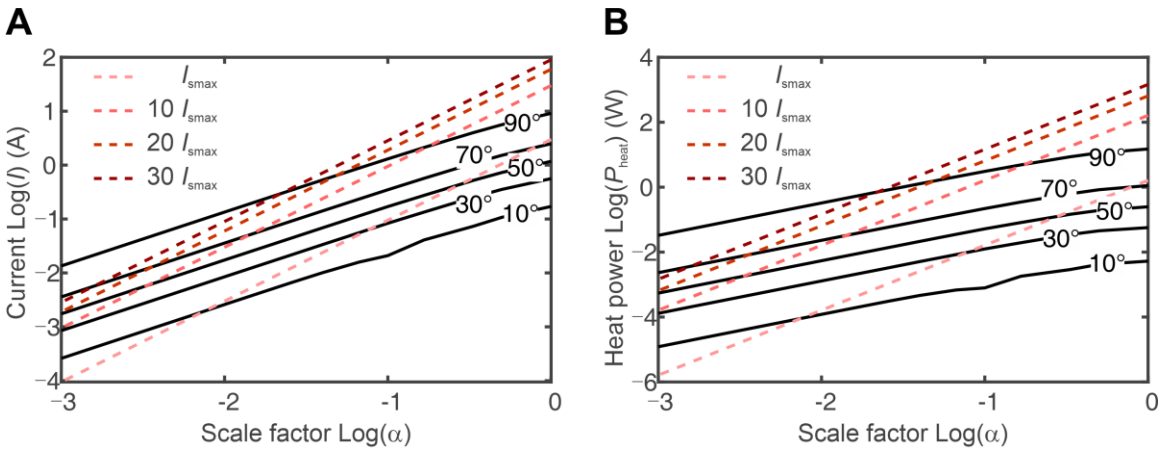

Fig. S7. Current and heat power consumption of scaled SEMAs. (**A**) Log-log plot of current and scale factor. (**B**) Log-log plot of heat power and scale factor. The black solid lines and the red dashed lines refer to the static bending angles (10°, 30°, 50°, 70°, and 90°) and the applied current I (1, 10, 20, and 30 I_{smax}), respectively.

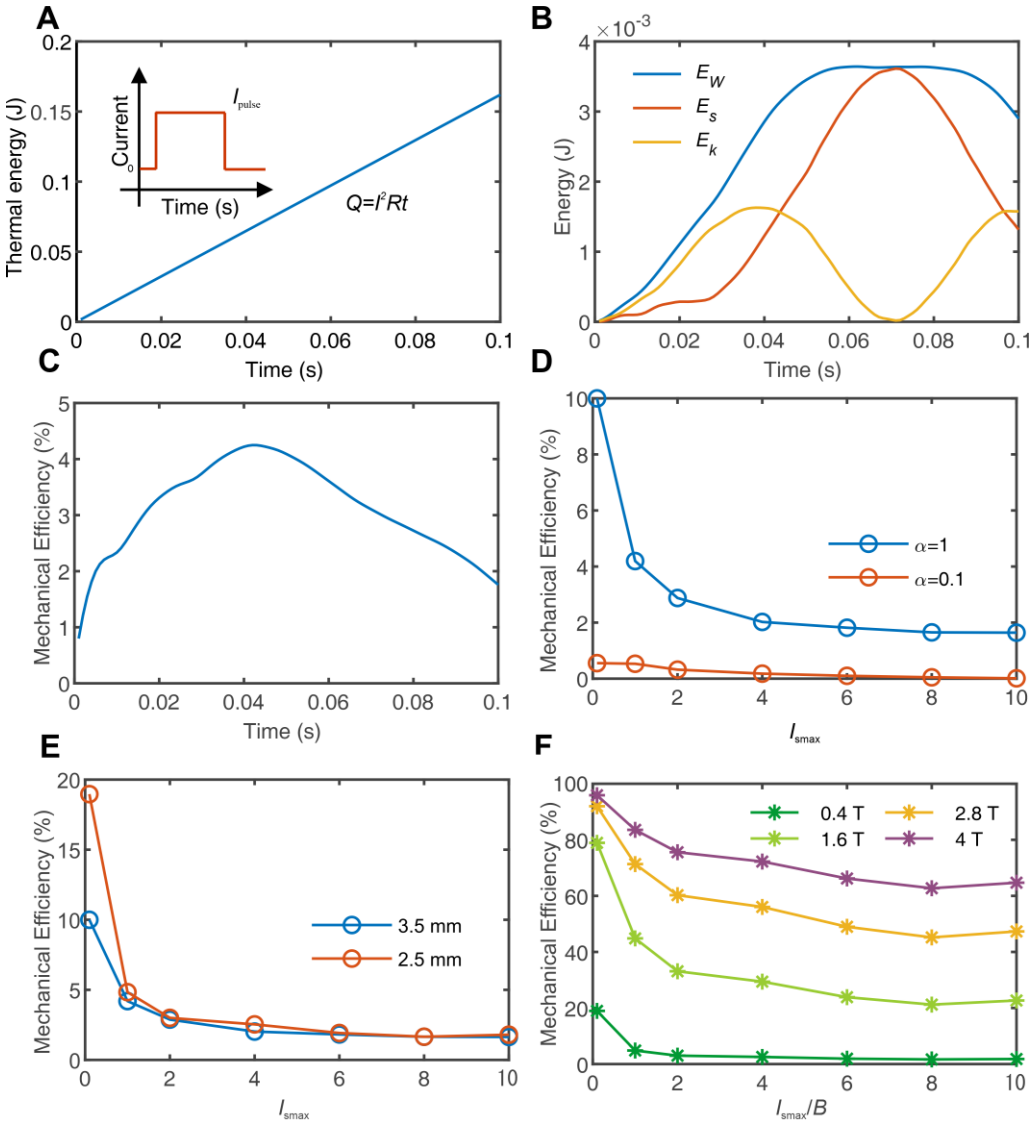

Fig. S8. Efficiency analysis of SEMAs. (**A**) Thermal energy generated by the SEMAs. The inset shows the schematic diagram of the applied current pulse. (**B**) Time-related variation of the mechanical work (E_w), strain energy (E_s), and kinetic energy (E_k) of SEMAs. (**C**) Variation of mechanical efficiency *vs.* time. (A), (B) and (C) are obtained from the response of the reference single-coil square SEMA subjected to a 3 A pulse lasting for 0.1 s. (**D**) and (**E**) are the maximum mechanical efficiencies of SEMAs with different sizes and thicknesses, respectively, subjected to various currents. (**F**) Maximum mechanical efficiency *vs.* specific current (I_{smax}/B) of a 2.5-mm-thick single-coil square SEMA subjected to magnetic fields B ranging from 0.4 T to 4 T. In (D), (E) and (F), the currents we used are 0.1, 1, 2, 4, 6, 8, and 10 times of I_{smax}.

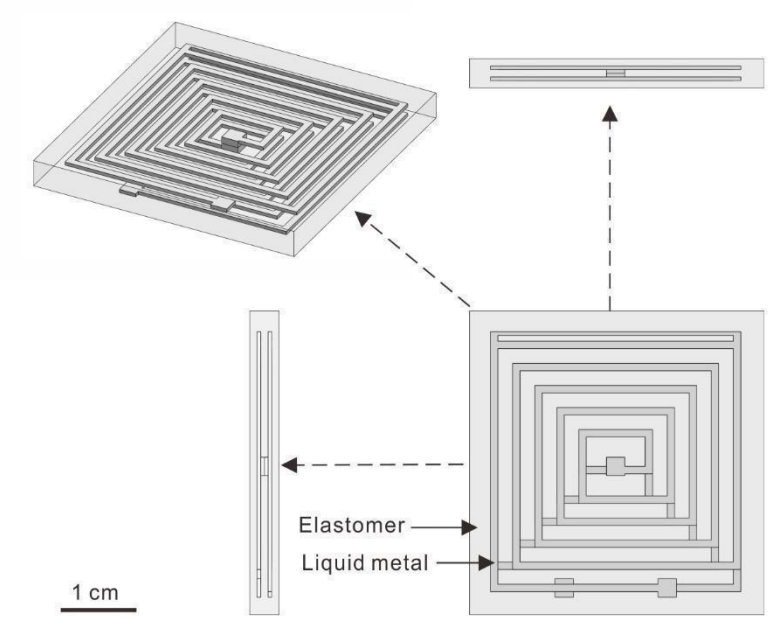

Fig. S9. The structure of a double-coil square SEMA from different angle views.

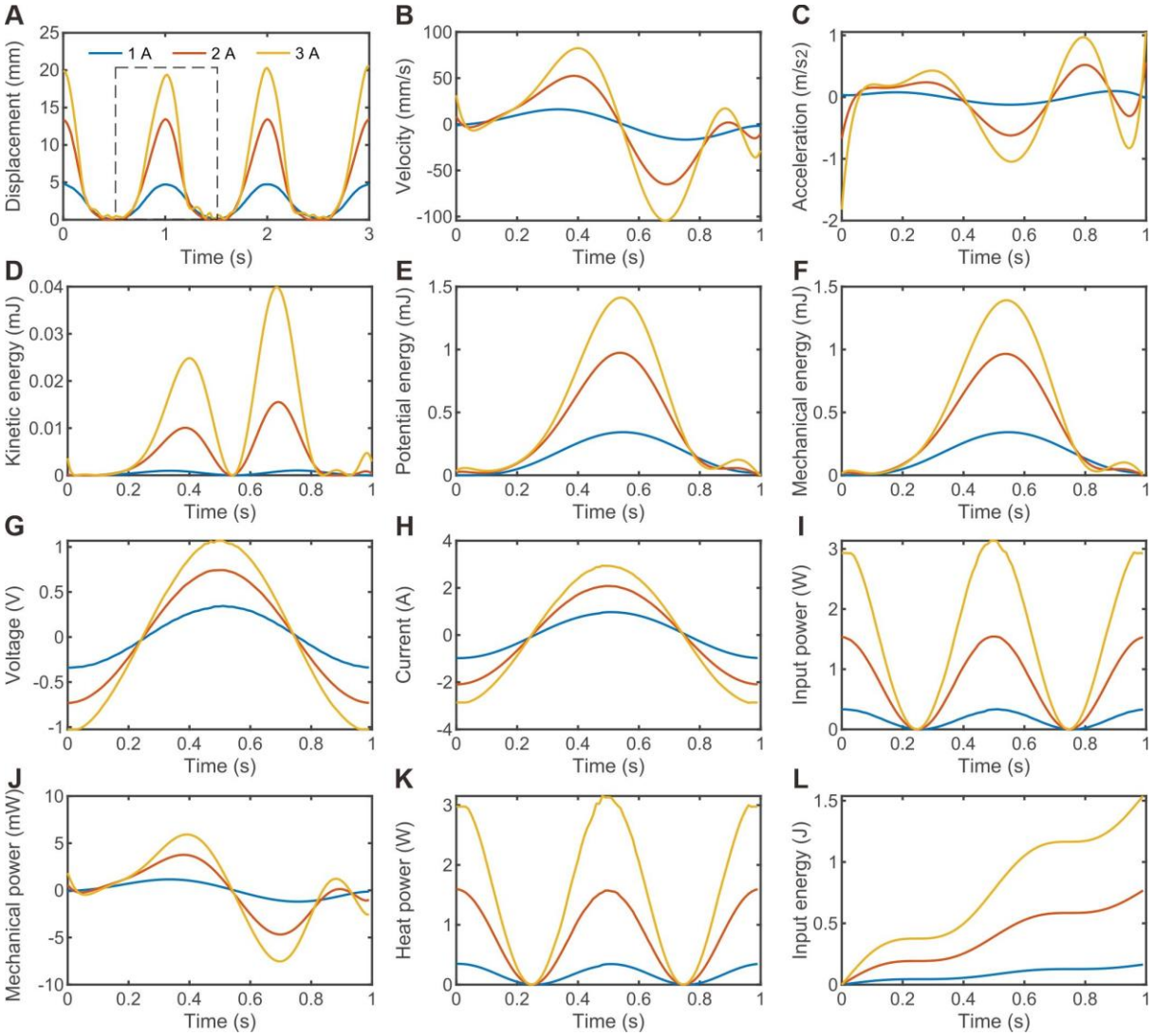

Fig. S10. Characterization of a double-coil square SEMA lifting a weight. (**A**) The displacement *vs.* time of the weight for three periods (Movie S5). (**B**) The velocity, (**C**) acceleration, (**D**) kinetic energy, (**E**) potential energy and (**F**) mechanical energy *vs.* time of the weight in one period. (**G**) The voltage, (**H**) current, (**I**) input power, (**J**) mechanical power, (**K**) heat power and (**L**) input energy *vs.* time of the SEMA for one period.

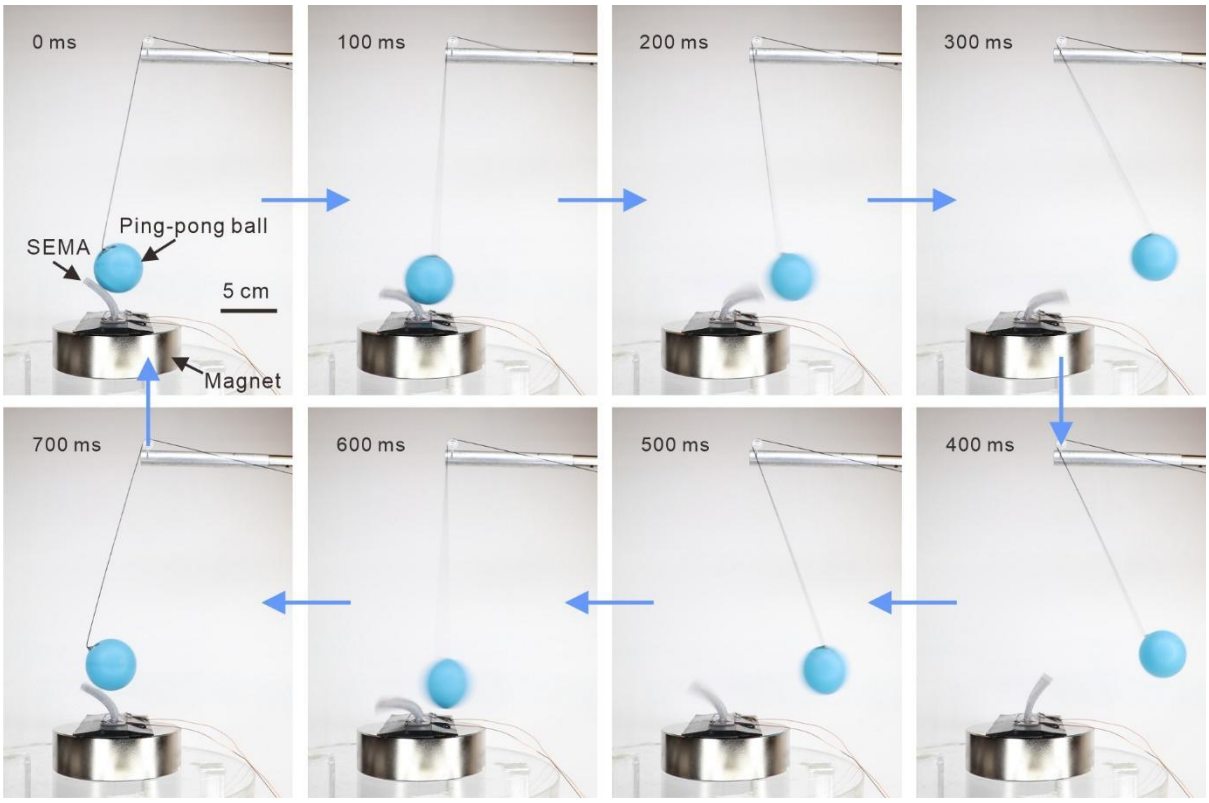

Fig. S11 Snapshots of a double-coil square SEMA playing ping-pong with a ball. The SEMA is driven by a square wave current with 1 A @ 1.5 Hz. (Movie S6). (Photo Credit: Michael Drack and Guoyong Mao/Johannes Kepler University Linz).

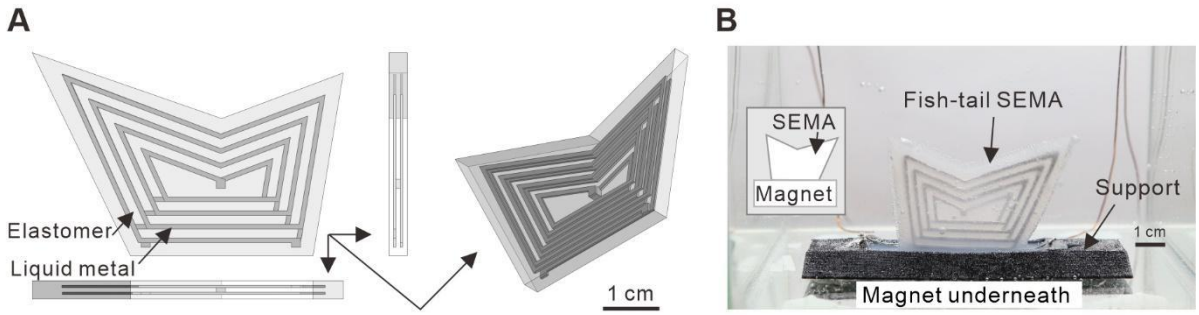

Fig. S12. Design and experimental setup of a fish-tail SEMA. (**A**) The geometry of the fish-tail SEMA. (**B**) Experimental setup for characterizing the fish-tail SEMA immersed in water. (Photo Credit: Michael Drack and Guoyong Mao/Johannes Kepler University Linz).

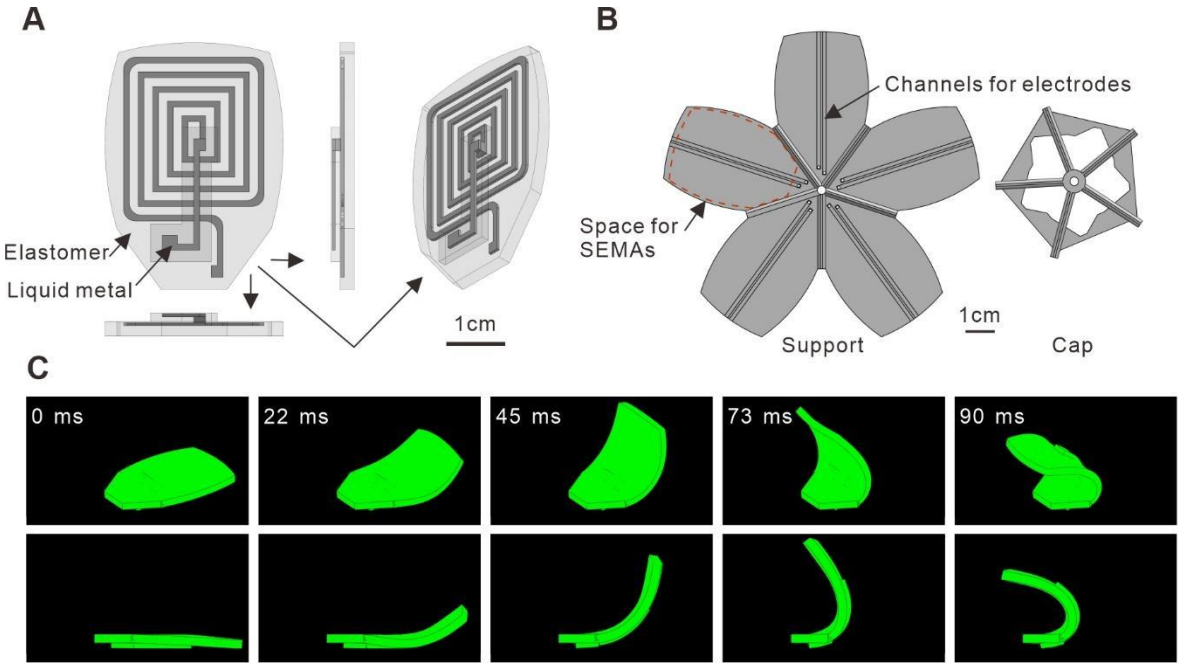

Fig. S13. Design of the flower SEMA. (**A**) Structure of one petal of the flower SEMA. (**B**) Design of the support of the flower SEMA. (**C**) Dynamic simulation of a single petal subjected to a current switching from 0 to 5 A. The bottom row shows the deformation of the SEMA from side view (Movie S8).

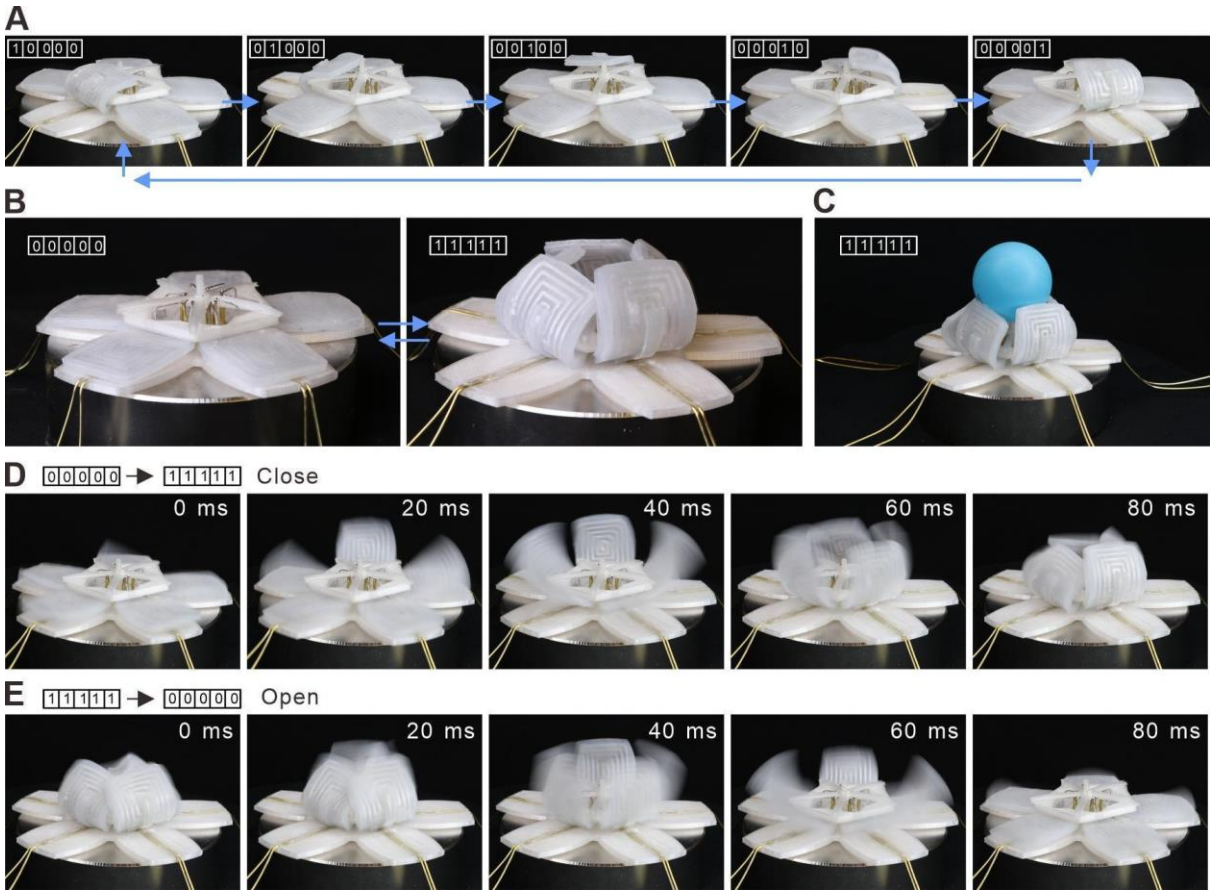

Fig. S14. Actuation of the flower SEMA assembled from five individual petals. (**A**) Closing and opening of each petal in a sequence. (**B**) Closing and opening of the whole flower (all five pedals) by switching the power. (**C**) The closed flower gently holding a ping-pong ball. (**D**) Fully closing the flower in 80 ms. (**E**) Fully opening the flower in 80 ms (Movie S8). (Photo Credit: Michael Drack and Guoyong Mao/Johannes Kepler University Linz).

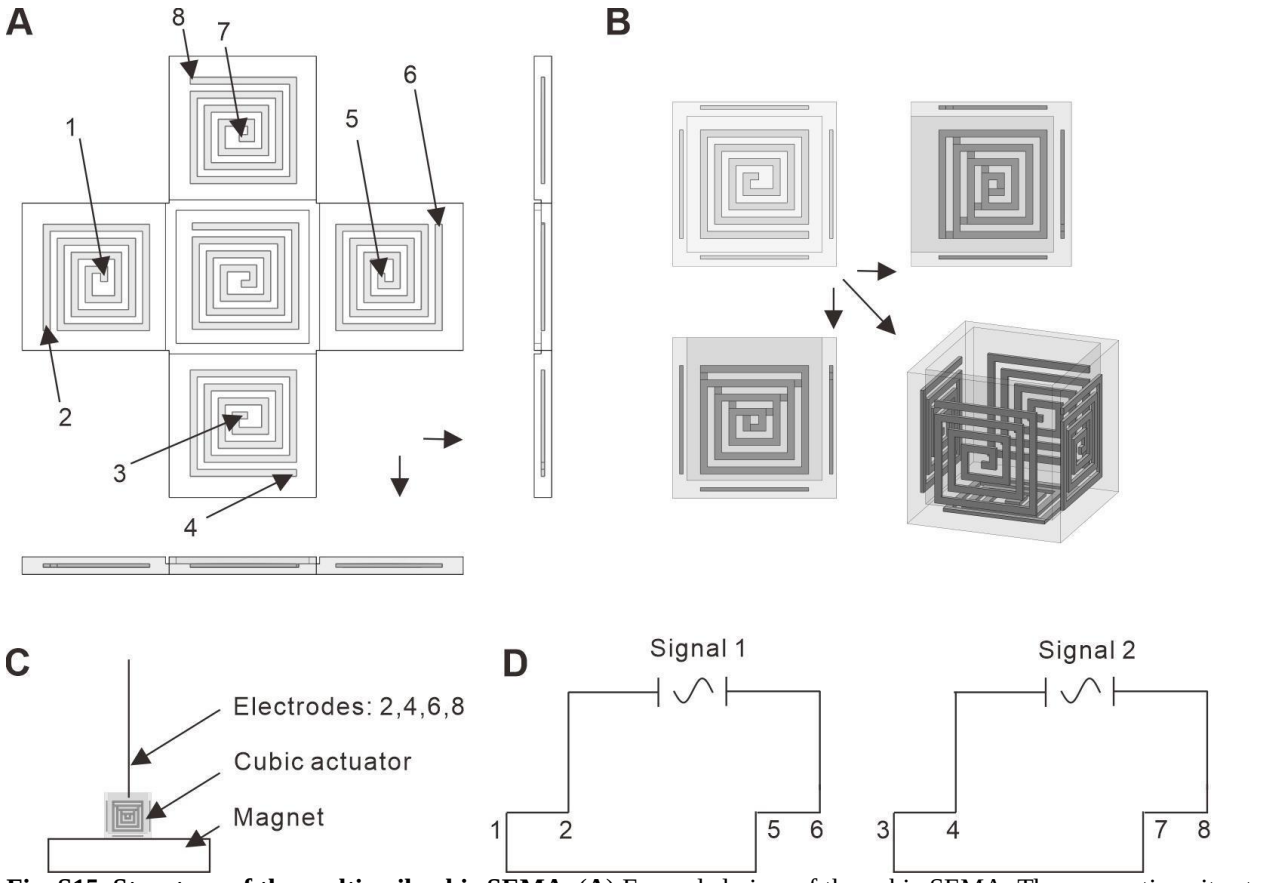

Fig. S15. Structure of the multi-coil cubic SEMA. (**A**) Expanded view of the cubic SEMA. The connection sites to the power supply are labeled with numbers. (**B**) Folded cubic SEMA from different perspectives. (**C**) Experimental setup for testing the cubic SEMA. The connection sites 2, 4, 6, 8 are connected to the control system. (**D**) The connection of the cubic SEMA to the control system. Opposite surfaces of the cubic SEMA are connected in series.

P_{ij}						
i / j	0	1	2	3	4	5
0	0.002769	-0.7488	-14.47	2961.0	-4.231e+04	-2.24e+05
1	2.501	354.7	-2.49e+04	2.71e+05	2.785e+06	
2	-94.66	6693.0	3.79e+05	-1.324e+07		
3	3533.0	-4.705e+05	1.23e+07			
4	2.407e+04	-2.656e+06				
5	3.864e+05					
Q_{ij}						
i / j	0	1	2	3	4	5
0	0.3575	0.7711	-43.96	-1.019e+04	2.872e+05	-2.118e+06
1	0.6745	-587.6	4.608e+04	-1.082e+06	7.551e+06	
2	692.1	-5.846e+04	1.303e+06	-6.506e+06		
3	2799.0	2297.0	-6.716e+06			
4	-3.788e+04	7.097e+06				
5	-2.499e+06					

Table S1. Parameters for fitting the magnetic fields with 2D polynomials. Note: we use E-notation that means 'MeN' indicates '$M \times 10^N$'.

Number	Height (*Z*, mm)	Length (*l*, mm)	Direction of current
1	3.5	22.25	-1
2	6.5	30	-1
3	9.5	24	-1
4	12.5	18	-1
5	15.5	12	-1
6	19.5	3.25	-1
7	24.5	9	1
8	27.5	15	1
9	30.5	21	1
10	33.5	27	1
11	36.5	33	1

Table S2. The dimensions of the channels in the single-coil square SEMA.

Category	Response time (s)	Controllability ***	Energy density† (J/cm^3)	Efficiency	Power Source	Miniaturization	Drawback/ limitation
Humidity-driven actuator (*1*)	~600**	Difficult	/	/	Humidity	Easy	Slow response
pH-responsive actuator	~360**	Difficult	/	/	pH	Difficult	Aqueous solution
Liquid crystalline elastomer actuators (*2-4*)	~60**	Moderate	0.01	Low	Light/heat	Easy	Slow response
Hydraulic/pneumatic actuators (*5*)	~ 2**	Moderate	/	Low	Fluid pressure	Difficult	High pressure
Shape memory polymer (*6, 7*)	~60**	Moderate	0.1	Low	Heat	Easy	Slow response
Soft magnetic actuators (*8*)	~1×10^{-3}*	Moderate	0.02	/	Magnetic field	Easy	High precise magnetic field
Dielectric elastomer (*9*) /hydraulically electrostatic actuators (*10, 11*)	~1×10^{-3}*	Easy	1	High	Electric field	Difficult	High voltage
SEMAs(*12, 13*)/Our work	~1×10^{-3}*	Easy	0.49††	High††	Current, Magnetic field	Easy	Strong magnetic field

*The value can be higher (as a loudspeaker), here for simplicity, we use 1×10^{-3} s.
**Depends on the size of the actuator and difference of the stimuli between actuator and environment.
*** Controllability includes the precision in control and the programmability.
† Calculation only considers the actuator.
†† With high magnetic field.

Table S3. Comparison of SEMAs with current popular soft actuators.

Movie S1. A swimming soft shark driven by SEMAs.

SEMAs act as tail and fins. The driving current is a square wave with 3 A @ 4 Hz. The fish is put at the center of the magnet with the axis of the fish along the asymmetric axis of the plate magnet. Turning the current on and off drives the shark through the water (see Fig. 1B, Fig. S2)

Movie S2. Stretchability of a SEMA.

A single-coil square SEMA is stretched randomly by hand up to 220% proofing the stretchability of the soft actuator. Furthermore, the video shows that the liquid metal channels are well sealed even under stretch (see Fig. S4E&F).

Movie S3. Bending of a single-coil square SEMA in experiment and simulation.

The video shows the experimental and simulated results also presented in Fig. 2A&B. The simulation in the video is continuously composed of 100 static pictures (green outlined). The experiment in contrast is composed only of 13 static pictures.

Movie S4. Dynamic tests of a single-coil square SEMA.

In the test a square wave current is applied to the SEMA. We excite the SEMA with different frequencies from 1 to 10 Hz with a step of 1, and from 2^{10} to 2^{14} with a scale factor of 2. At a frequency of 2^{14}, the sound from the SEMA is no longer audible to the human ear.

Movie S5. A double-coil square SEMA lifts a load.

The SEMA is connected to a weight with a thread via a deflection pulley. By switching the DC current from -3 A to 3 A, the SEMA bends from one to the other side and lifts the weight of 7.32 g by 2 cm (see Fig. 3A).

Movie S6. A double-coil square SEMA plays with a ping-pong ball.

A double-coil square SEMA hits a ping-pong ball hanging on a thread like a simple pendulum. By applying a current pulse from –3 A to +3 A, the SEMA pushes the ball 47 mm into the air. Sourcing a square wave current of 1 A @ 1.5 Hz results in a periodical ping-pong play (see Fig. 3E, Fig. S9).

Movie S7. Function of a fish-tail SEMA.

A fish-tail like SEMA is placed at the bottom of a water tank to demonstrate the safe operation in water without additional isolation due to the low driving voltage (<1 V). A magnetic field applied by a plate magnet placed underneath the tank (Fig. S10), lets the SEMA swing like a fish-tail when applying a 3 A square wave current. The solid blue dye dripped into water at the beginning of the experiment is rapidly mixed depicting the high performance of the SEMA (see Fig. 4B).

Movie S8. A programmable flower SEMA.

The multi-coil flower SEMA consists of five single pedals that can be controlled individually. Dynamic simulation of a single petal subjected to a current switching from 0 to 5 A shows the deformation of one single pedal (Fig. S11). Furthermore, the single petals are actuated sequentially as well as all of them simultaneously. The petals are actuated one by one with a time interval of 10 ms, 50 ms, 100 ms and 1 s showing the outstanding dynamic performance of our SEMAs (see Fig. 4C&D, Fig. S12).

Movie S9. A cubic SEMA rotating in xy-plane.

Only two opposing faces were actuated simultaneously in the video (Fig. S13D). We used a pulse current (100 ms, 10 A) to rotate the SEMA. By choosing the actuated faces and the current, it is able to control the rotation of the SEMA (see Fig. 4E).